14th International Conference on Structural Safety and Reliability - ICOSSAR'25
1-6 June, 2025 - Los Angeles California, USA
R. Ghanem, E. Johnson, S. Masri and A. Olivier (Eds)

BAYESIAN UNCERTAINTY ANALYSIS OF GROUTED ANCHORS

MORITZ J. P. EFFENBERGER[1], CHRISTIAN MOORMANN[2]

[1] Institute for Geotechncial Engineering, University of Stuttgart
Pfaffenwaldring 35, 70569 Stuttgart, Germany
moritz.effenberger@igs.uni-stuttgart.de

[2] Institute for Geotechncial Engineering, Head of Chair, University of Stuttgart
Pfaffenwaldring 35, 70569 Stuttgart, Germany
christian.moormann@igs.uni-stuttgart.de

Key words: Bayesian, Uncertainty, Capacity, Reliability, Anchor, Covariance

Abstract. This research proposes a data-driven, Bayesian framework to obtain reliability and pull-out capacity estimates of individual grouted anchors, using suitability and investigation test data. Two covariance modeling approaches were investigated, the first quantifying the total uncertainty of model and data, the second specifying measurement/observation uncertainty and model uncertainty separately. Both methods deliver plausible predictions, providing, with the probability of failure an additional criterion on which grouted anchors can be assessed. Additionally, the estimated pull-out capacity distributions from suitability tests were in line with measured pull-out capacities obtained from investigation tests, verifying the approach.

1 INTRODUCTION

Grouted anchors are versatile structural elements in geotechnical engineering, bearing tensile loads of a variety of structures and transferring these into the adjacent soil. Their bearing behavior is highly uncertain due to spacial variability, installation effects, and measurement inaccuracies. Exact design methods do not exist, only empirical or semi-analytical methods developed mainly in the early stages of anchor research in the 1970's [1, 2, 3] . Therefore, most common engineering practice is to carry out full-scale load tests of varying extent to verify grout anchor bearing capacity. Grouted anchor test conduct is regulated in ISO standard [4], categorized in investigation, suitability and acceptance tests, which are characterized by a decreasing extent in the mentioned order. Due to the anchors unique verification requirements, a lot of data is generated in the process. Current practice in design is usually to regard the lowest measured bearing capacity of an anchor group as the governing one, as the test results are used mainly for verification purposes. Therefore, uncertainties in the bearing behavior and reserves in the bearing capacity remain unquantified. Load test conduct for all of the aforementioned procedures is regulated in [4]. For testing procedure 1, this entails that the anchor is loaded, the load is held, and the displacement over time is measured. Since the geotechnical failure of grouted anchors lacks a distinct failure condition, their performance is assessed based on their creep behavior. This characteristic is summarized in the form of the creep coefficient, which is the gradient of the displacement curve on a logarithmic time axis, since the idealized anchor displacement would be linear in half-logarithmic space, eq. 1.

It is an ambiguous criterion because the time steps in which the measurements are taken are not fixed, but it is up to the interpreter to decide which gradient captures the behavior best. For a creep coefficient exceeding 2.0 mm, according to the European guideline [7, 8], the anchor is at failure and cannot support more load, as it slowly emerges from the ground. The creep coefficient as a performance indicator can be insufficient, especially in cases where the anchor is close to the failure limit according to the creep value, allowing only qualitative judgment apart from binary classification, either the anchor failed or it did not. A more objective measure is a reliability assessment by estimating a probability of failure. Opposed to a deterministic analysis, such a calculation allows the quantification of uncertainty in the model response by introducing these uncertainties in the form of the parameters probabilistic distribution functions [9, 10, 11]. For geotechnical parameters uncertainty is mainly composed of measurement and transformation uncertainty [12]. A common approach to model both, measurement and transformation uncertainty simultaneously is to model their coefficient of variation as a random variable [13, 14]. For the case of anchor measurement over time, independence is assumed over each taken measurement. Many geotechnical applications of uncertainty quantification deal with spacial measurements [15], which is why these models cannot be applied directly to the problem at hand, where covariance over time needs to be computed. Furthermore, depending on the type of measurement and its characteristics, the appropriate choice could be either a multiplicative, as in [16], simulating vane shear tests with corresponding error or as additive error [17], depending on the physical process underlying the measurement proceeding. The governing sources of uncertainty identified regarding the modeling of individual anchors are observation (measurement) and model uncertainty. For this type of measurement, anchor head displacement over time, additive measurement error is considered to the most reasonable choice.

Since transformation error does not apply with the problem at hand, the second source of uncertainty is model error or model inadequacy. Such quantities are commonly captured using a multiplicative error formulation [18, 13, 16]. For one-dimensional measurements, this entails that all values of the vector are multiplied by an single error term. In [19], an overview of different error models can be found, focusing on mixed model, meaning both additive and multiplicative formulations are combined. Further mathematical insights in formulating mixed error models can be related in [20]. A multiplicative error formulation has been investigated but was found to be inappropriate for the model at hand, because due to the nonlinear displacement curve physically unrealistic displacement curves were obtained and therefore discarded. The faulty results were chosen not to be reported.

This research aims to investigate different modeling approaches to quantify observation and modeling uncertainty of investigation and suitability test data. Uncertainty quantification was conducted by a Bayesian analysis comparing two different covariance models. Based on posterior and posterior predictive results, reliability and pull-out capacity estimates were obtained.

2 METHODS

The data used in this research stems from grouted anchor suitability and investigation tests, conducted according to ISO [4] testing procedure 1. Each anchor is loaded and unloaded stepwise, while the load is being held for a specific time period, which depends on the soil conditions, longer for cohesive soils, shorter for non-cohesive soils. During this time period the displacement is measured to observe the anchors creep characteristics. Based on the creep coefficient (Eq. 1), the performance of the anchor is assessed.

$$k_s = \frac{s_2 - s_1}{\log(\frac{t_2}{t_2})} \tag{1}$$

Two case studies are investigated, case study 1 consists of nine anchors, each anchor loaded in five load steps, conducted as suitability tests, with the similar soil conditions for each anchor, with their grout body built in claystone. Case study 2 consists of three anchors, which were first tested on their suitability in five load steps. In a later stage of the project, the tests were extended to investigation tests, performed on the same anchors. Generally, grouted anchor bearing behavior is uncertain and difficult to predict which is why guidelines, [4, 5, 6] advise conducting these extensive tests. However, the tests alone do not necessarily aid in the quantification of the total uncertainty, nor in the allocation of the source. A useful tool for statistical uncertainty quantification is Bayesian analysis.

This statistical method enables the calculation of parameters $\boldsymbol{\theta}$ distributions conditional on data $\boldsymbol{D}$ and prior knowledge $\boldsymbol{p_0}$ as the posterior distribution $P(\boldsymbol{\theta}|\boldsymbol{D})$ (Eq. 2) [21].

$$P(\boldsymbol{\theta}|\boldsymbol{D}) = \frac{P(\boldsymbol{D}|\boldsymbol{\theta}) \cdot P_0(\boldsymbol{\theta})}{P(\boldsymbol{D})} \tag{2}$$
$$P(\boldsymbol{\theta}|\boldsymbol{D}) = \frac{P(\boldsymbol{D}|\boldsymbol{\theta}) \cdot P_0(\boldsymbol{\theta})}{\int_{-\infty}^{+\infty} P(\boldsymbol{D}|\boldsymbol{\theta}) \cdot P_0(\boldsymbol{\theta})}$$

The probability $P(D|\theta)$ in Bayes Theorem (Eq. 2) is the likelihood function, which is formulated as a multivariate normal distribution,

$$P(\boldsymbol{D}|\boldsymbol{\theta}) = \frac{e^{\frac{1}{2}(M(\boldsymbol{\theta})-\boldsymbol{D})^T \boldsymbol{\Sigma}(\boldsymbol{\theta})^{-1}(M(\boldsymbol{\theta})-\boldsymbol{D})}}{\sqrt{(2\pi)^k |\boldsymbol{\Sigma}(\boldsymbol{\theta})|}} \tag{3}$$

In the context of this research, the random variable vector $\boldsymbol{\theta}$ consists of model parameters to an analytical model $M(\theta)$, capable of reproducing the load bearing behavior of an anchor and variance parameters necessary to estimate the covariance of the likelihood function, effectively quantifying the underlying uncertainty. The details to the statistical model are illustrated in Fig. 1. To capture the anchor head displacement mathematically and relate the data to parametric uncertainty, the analytical anchor head displacement model according to Montero-Cubillo et. al. [22] was used. The rheological soil parameters of this anchor model are treated as random variables. Since this is a data-driven approach, weakly informative prior knowledge of all random variables is used in the form of uniform distributions. In this context, uniform distributions imply that the larger and smaller soil parameters and thus displacements are conceivable, compared to what is observed. The covariance matrix in Eq. 3 is the key quantity to estimate the variance associated with the statistical model and governing the variance of the predictive model. In this research two different covariance models are investigated.

2.1 MODEL 1

The first model quantifies the total uncertainty in the form a variance parameter for each time step, corresponding to a measurement, without distinguishing different sources. An initial assumption is that there is no temporal correlation between the measurements - a large measurement in the beginning does not imply a large measurement at the end of the observation period. Therefore, the covariance is modeled as described in eq. 4, in the form of a diagonal covariance matrix.

$$\sigma_{i,0} = U(1e-10, 1e-2)$$
$$\Sigma = \sigma_i I \tag{4}$$

A simpler covariance model would be a single covariance term that does not change over the time axis, multiplied with an identity matrix. However, such a simplified model seemed to be inappropriate considering the strong non-linear anchor behavior, since the variance at each time step would be equal.

2.2 MODEL 2

The main contributing sources of uncertainty regarding this individual anchor model are observation uncertainty and model inadequacy/error. Observation error is modeled additive,

$$\begin{aligned} \sigma_{m,0} &= U(1e-10, 1e-2) \\ \varepsilon_{m,i} &= \mathcal{N}(0, \sigma_m) \end{aligned} \tag{5}$$

with $\varepsilon_{m,i}$ stemming from the same zero-mean Gaussian distribution for each time step. This way, the measurement error can be positive or negative at each time step while being sampled from the same underlying distribution, valid for one observation.

For the model inadequacy, a different approach to the discussed multiplicative model discussed in section 1 is chosen. Since the model has such a non-linear response, it was conceived that the model error should follow a trend, as it is increasing over time. Each error term $\varepsilon_{t.i}$, corresponding to a measurement data point, cannot be modeled as stemming from the same distribution for each time step, as for the observation error. However, introducing a separate standard deviation for each time step to sample from, implementing many random variables, seemed unpractical regarding the number of random variables in relation to data points of the observation. Therefore, the standard deviation of model error was implemented via an estimator function $e(t, m_t, \sigma_m)$ (Eq. 6), which describes the trend of standard deviation evolution over time instead of modeling it directly.

$$m_{t,0} = U(1e-10, 1e-2)$$

$$e(t, m_t, \sigma_m) = \sigma_t = m_t \cdot \log(t) + \sigma_m \tag{6}$$

$$\varepsilon_{t,i} = \mathcal{N}(0, \sigma_{t,i}) \tag{7}$$

$$\Sigma = \varepsilon_m^2 + \varepsilon_t^2 \tag{8}$$

$$\hat{y} = \mathcal{M}(\theta) + \varepsilon_m + \varepsilon_t \tag{9}$$

After initial investigation, a log-shaped estimator function was chosen among a linear and exponential trend, since it captured the behavior best and its convergence was not influenced by the limits of its prior but proved most robust. No correlation between the error terms is assumed. The plate diagram in figure 1 summarizes the statistical model.

2.3 POSTERIOR PREDICTIVE & EXTRAPOLATION

The Bayesian analysis is computationally intensive. In this context, the analysis is carried out relying on samplers of the Markov-Chain-Monte-Carlo class. Analytical solutions to Bayes Theorem are only available for conjugate distributions [21]. In the case of this analysis, no conjugate formulations are available, which is why a numerical solution using the aforementioned samplers must be obtained. The analyses have been conducted with the No-U-Turn-Sampler (NUTS) [23], which is implemented in the open-source python library “pyMC”. As the model becomes more complex, from model 1 to

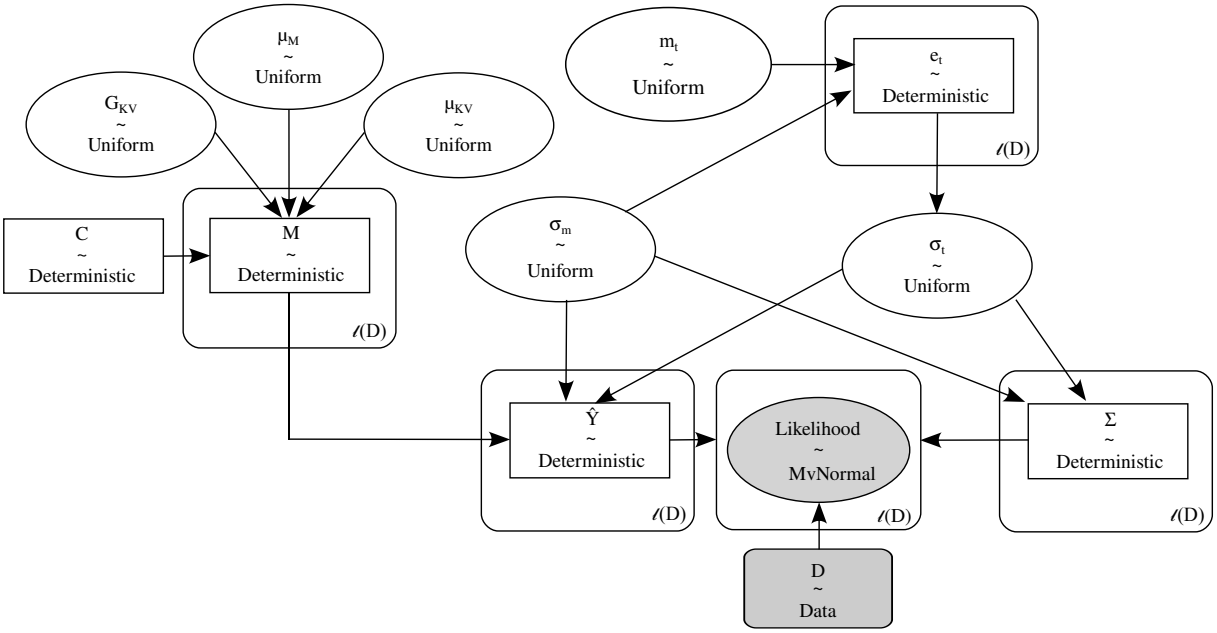

Figure 1: Plate Diagram Model 2

model 2, the blackjax implementation of NUTS was used, increasing the computational performance by calculating on the GPU instead of the CPU. Once the posterior distribution is calculated based on these model variations, the posterior-predictive distribution is evaluated.

$$P(D'|D) = \int_{-\infty}^{+\infty} P(D'|\theta)P(\theta|D)d\theta \tag{10}$$

By utilizing samples from the posterior-predictive distribution, which serve as statistically plausible displacement curves, the creep coefficient distribution can be estimated. Based on the creep distribution samples, the anchor's reliability can be estimated utilizing the conjugate beta-binomial model according to [24]. This way, the uncertainty in the reliability estimate is quantified, especially of advantage if no samples or just a few lie in the failure domain. The failure domain is defined based on the limiting creep coefficient, here chosen to $k_{s,lim} = 2.0$ mm according to [7]. Apart from reliability assessment, the anchors geotechnical pull-out capacity can be estimated utilizing the creep distribution estimate. For grouted anchors, their creep coefficient evolution for increasing load tends to develop exponentially [1]. This characteristic can be leveraged by fitting a non-physical exponential function (Eq. 11) to the estimated creep curves, consisting of the creep distribution samples for each load step of the test and evaluating the function at the failure limit of 2.0 mm.

$$k_s(P) = b(e^{aP} - 1) \tag{11}$$

The parameters a and b are empirical, non-physical fitting parameters and need calibration. Doing so for each posterior-predictive sample curve, an estimate is provided of the anticipated pull-out capacity distribution, which can be used for reliability analysis of the anchored structure which is investigated. The general framework can be related in Fig. 2 .

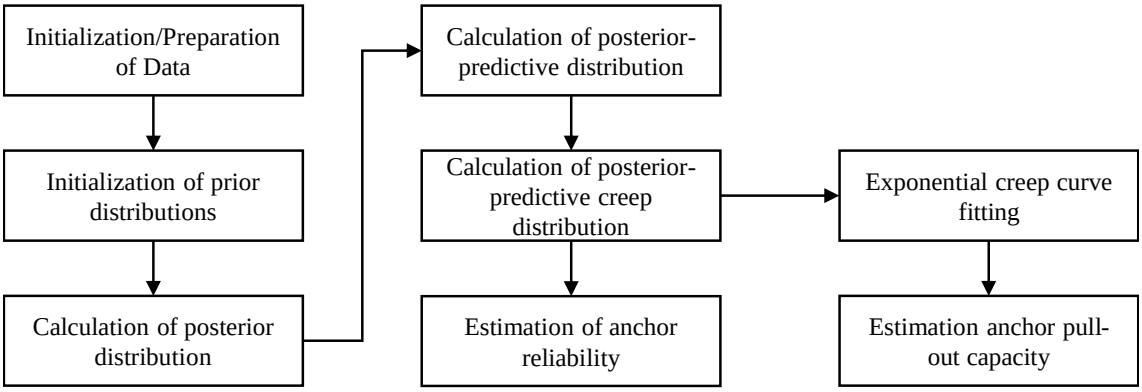

Figure 2: Procedure of analysis

3 RESULTS

3.1 POSTERIOR DISTRIBUTION

First, the marginal posterior results, according to eq. 2, are presented in fig. 3 **a**, **b**, **c**, depicting the marginals of the rheological soil parameters necessary to calculate the model response according to [22].

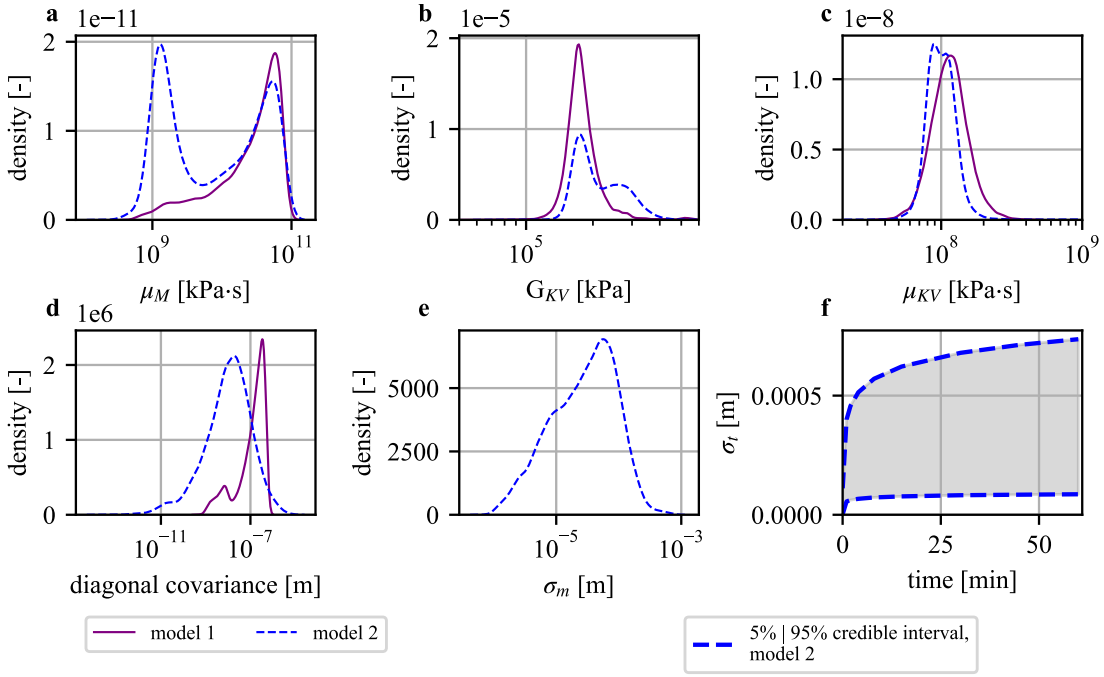

Figure 3: Marginal posterior distributions, case study 1, anchor 4

The distribution estimates differ mainly for the Maxwell viscosity (Fig. 3 **a**), where model 2 converges to a multi-modal distribution, while model 1 converges to the upper mode, close to the bound set by the prior. The possibility of non-unique solutions of the analytical displacement model

aggravate the interpretation of the marginals, especially if one tries to infer about the anchor behavior. These results are necessary for the calculation of the posterior-predictive distribution. Nevertheless, the marginals need to be inspected for to detect inconsistencies and problems in convergence.

Fig. 3, **d**, **e**, **f** show the marginal posteriors of the variance parameters. The general magnitude of the variances (fig 3, **d**) is the largest for the total error model, as it does not stretch out in to the smaller magnitude areas, exhibiting a denser distribution. Measurement error standard deviation σ_m (fig 3, **e**) and model error standard deviation σ_t (fig 3, **f**) are depicted. Both error terms are in reasonable dimensions as expected. The model error is governing the total variance while the measurement error is comparably small.

3.2 POSTERIOR PREDICTIVE DISTRIBUTION

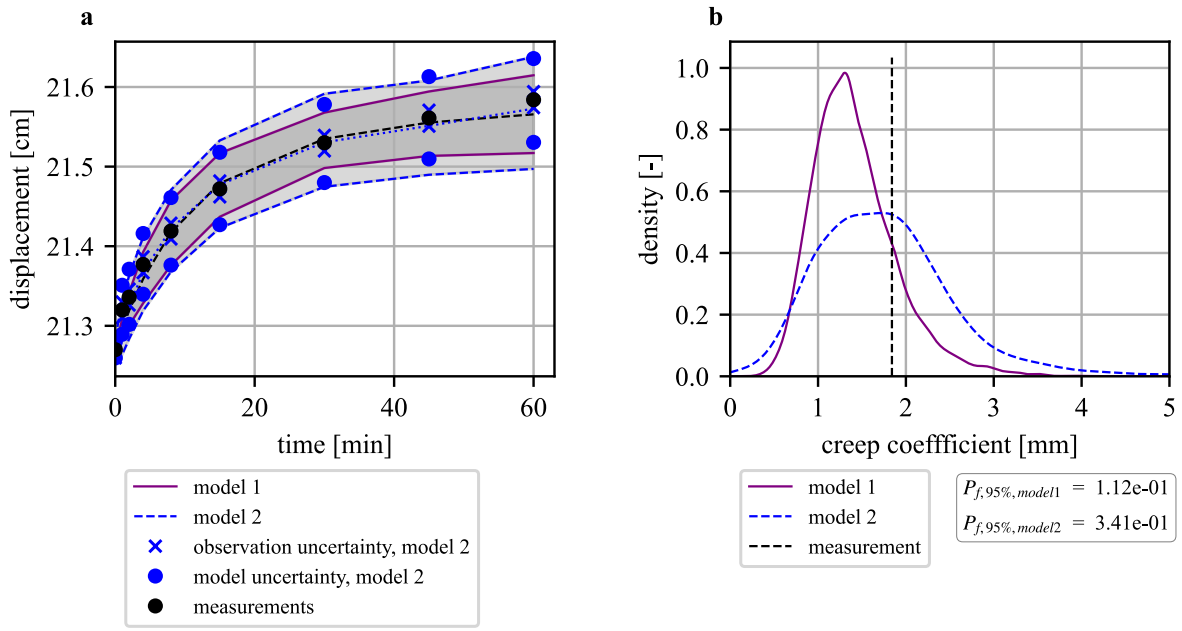

Figure 4: Posterior-predictive distributions, case study 1, anchor 4

For the posterior-predictive, model 1 and model 2 indicate more accordance, than one could expect by judging the marginal posterior distributions and their divergences. The total error model indicates marginally smaller credible bounds, compared to the uncorrelated error model (Fig. 4 **a**, 5 **a**). Their main difference lies in their gradients, summarized by the creep coefficient distribution (Fig. 4 **b**, 5 **b**). While both methods provide a reasonable estimate of the creeps distribution compared to the measurement, the total error model systematically underestimates creep, even considered its lognormal shape. The probabilities of failure, calculated as 95% credible intervals, are in a similar range, though the sensitivity becomes evident regarding the small differences in the posterior predictive distribution's variance.

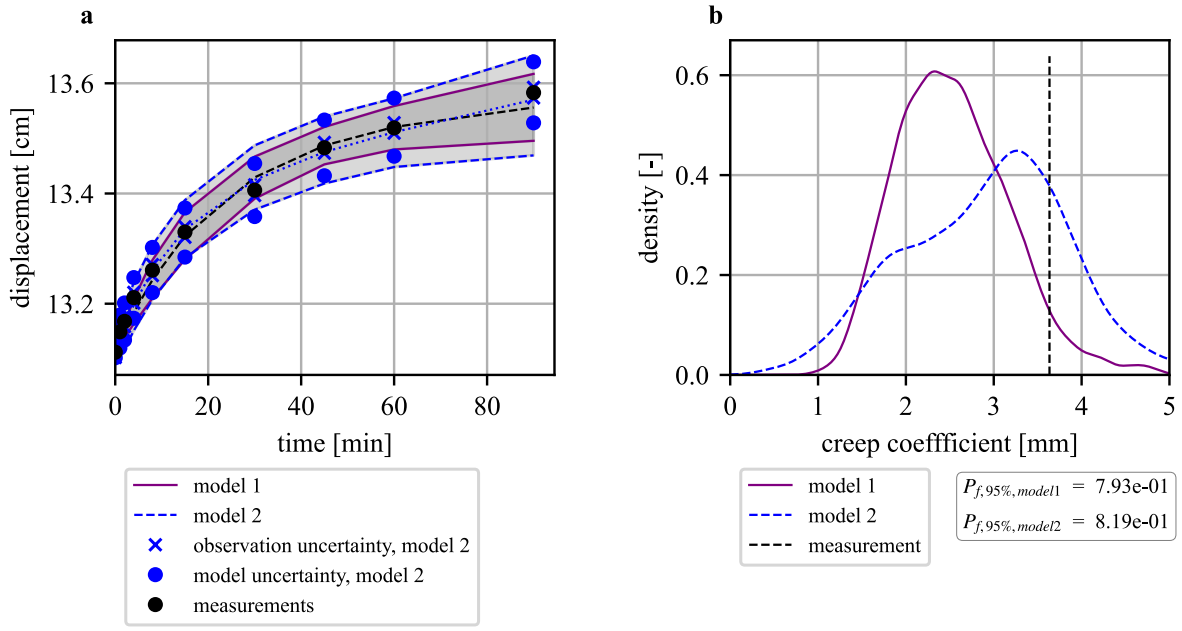

Figure 5: Posterior-predictive distributions, case study 2, anchor 3

3.3 POSTERIOR PREDICTIVE CREEP EXTRAPOLATION

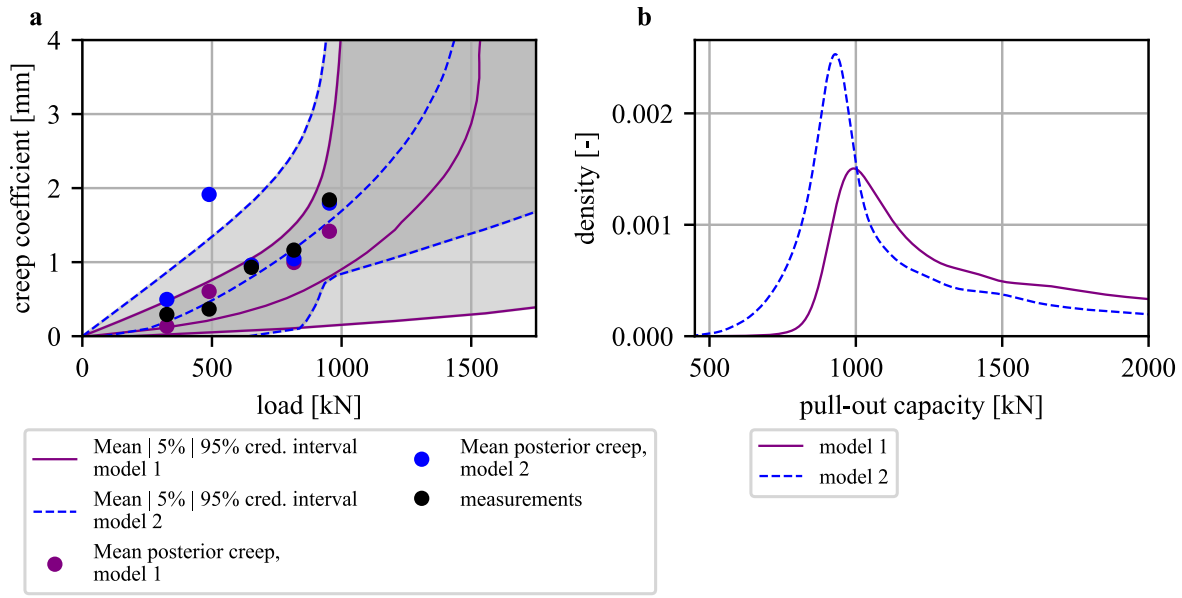

Figure 6: Posterior-predictive extrapolation, case study 1, anchor 4

The creep curve extrapolation model enables a prediction of the pull-out capacity. The credible bound curves (Fig. 6 **a**, 7 **a**) illustrate what range of values the predictions take for which loading conditions. While fig. 6 displays the prediction only for a suitability test, the exponential shape and the

resulting pull-out capacity (Fig. 6 **b**) shows more variance in the log-normally shaped distributions, compared to the investigation tests in fig. 7.

Especially the strong tails are wide and far reaching, as expected for such a nonlinear model. Also, the prediction of model 1 and model 2 diverges and seems to converge to a similar solution regarding the weak tails only for loads larger than the one applied.

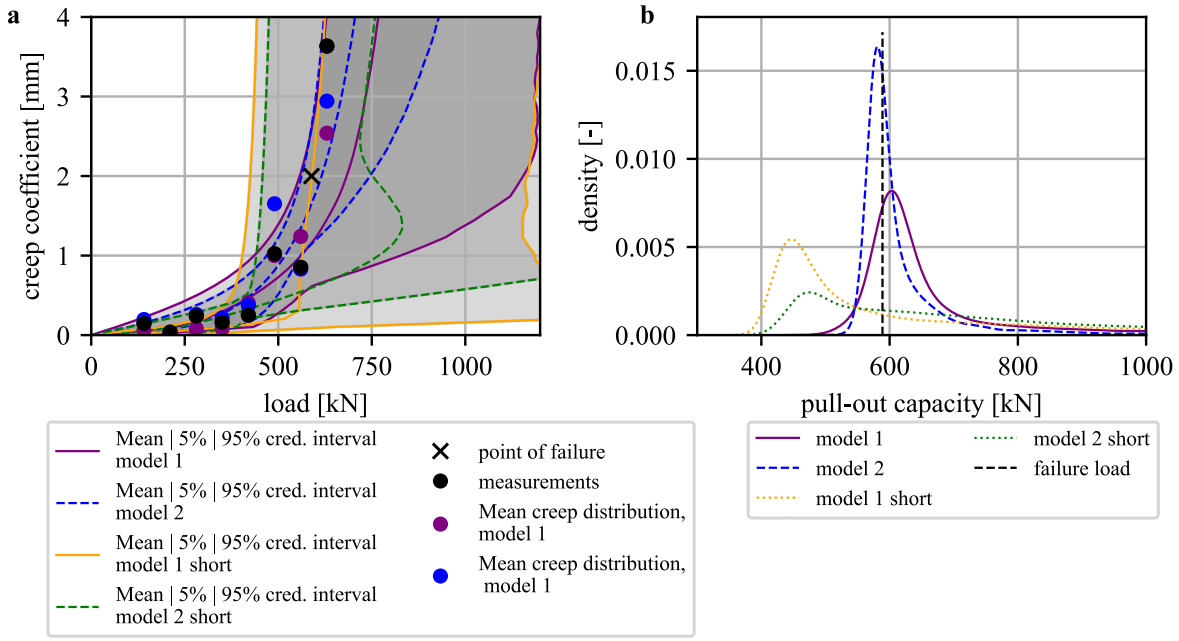

Figure 7: Posterior-predictive extrapolation, case study 2, anchor 3

The predictions of the suitability tests (labeled as 'short') aiming to reach a similar prediction as the investigation tests (Fig. 7) underestimate the achieved pull-out capacity in their mode (Fig. 7 **b**). The suitability tests' modes are significantly smaller than the measured pull-out capacity, located adjacent to the last applied loading condition on the x-axis. However, their mean values lie closer to the measured failure load (Fig. 7 **a**), while the distributions themselves show variance larger by several magnitudes, compared to the corresponding investigation test distributions.

4 DISCUSSION

The marginal posterior distributions indicated divergences between model 1 and model 2. The distributions partly exhibited different modes, however for most observations, the rheological soil parameters exhibited the similar modes with slightly different variance and tails. Their interpretation regarding the anchor behavior was difficult since the parameters themselves did not allow such judgment respectively. The covariances determined by model 1 were larger, which leads to more variance propagation. While the shown credible bounds of the posterior-predictive are narrower compared to model 2, the creep coefficient distributions and pull-out capacity distribution were wider. While the divergences in the marginal posterior distributions were more pronounced, the credible bounds of the posterior-predictive diverged in the magnitude of millimeters. With the creep coefficient distribution as the main quantity of interest, the reliability estimate and the pull-out capacity distribution depend

on an accurate estimate of the creep coefficient. Therefore, a good fit to the creep measurement is considered a quality assessment criterion of the model and its prediction.

Since model 1's posterior distributions hint to convergence issues, this model is considered less robust and since more effort needs to be spend on calibration of the prior distribution limits to achieve credible results. Model 2 was observed to be the more robust, consistently delivering credible results, while also quantifying observation error and model error in the form of their respective distribution functions, which was the aim of this analysis.

The posterior creep extrapolations divergences between both models can be appointed to the divergent creep coefficient distributions. The more accurate the posterior predictive creep distributions can match the corresponding measurement, the more credible the estimated pull-out capacity can be judged. In this regard model 1 indicates more weaknesses, since closer coinciding means with the measurement are predominantly found with model 2.

5 CONCLUSIONS

Two covariance models, part of a Bayesian analysis were presented to estimate grouted anchor reliability based on the posterior predictive creep coefficient distribution and the pull-out capacity based on an empirical, non-physical creep extrapolation model. Covariance model 2 additionally enables the estimation of measurement and model uncertainty, while model 1 solely quantifies the total uncertainty.

The anchors probability of failure serves as an additional measure of grout anchor assessment, beneficial for anchors tested to be close to its geotechnical failure criterion.

Pull-out capacity estimation and its underlying uncertainty in the form of its probability density function is necessary to perform reliability analyses of retained structures. The incorporation of suitability and investigation tests makes optimized use of knowledge which is available.

Both models show weaknesses in the prediction of the highly sensitive creep coefficient, leading to an propagation of the allocated variances in all following steps of the analysis. Other initial investigations showed, that considering the creep coefficient in the data vector as a separate measurement improves creep distributions estimates drastically. Problematic is the incorporation of this measurement in to the measurement error model - a topic for future research. Other limitations are the associated with the extrapolation itself, introducing further model error, which remains unquantified in the scope of this analysis. Furthermore, the data quality is governing in the extrapolation, relying fully on the idealized exponential trend, which is not always observable dealing with real data.

In future research, the incorporated framework is supposed to be improved regarding the predictive certainty of the posterior predictive creep coefficient distribution. Additionally, the framework needs to be extended to include the hierarchical structure of grouted anchor test data, allowing for a separate quantification of measurement uncertainty, model uncertainty and another spatial uncertainty component, capturing spatial variability and installation effects.

REFERENCES

[1] Ostermayer, H. Construction, carrying behaviour and creep characteristics of ground anchors. *Diaphragm walls and anchorages*. (1975), pp. 141–151.

[2] Littlejohn, G.S. *Ground Engineering*. In: Proceedings of the Conference organized by the Institution of Civil Engineers in London. (1970), pp. 33–44.

[3] James, E.L., Phillips, S.H.E. Movement of a tied diaphragm retaining wall during excavation. *Ground Engineering*. pp. 14–16.

[4] International Organization for Standardization. *ISO 22477-5:2018 Geotechnical investigation and testing — Testing of geotechnical structures - part 5: Testing of grouted anchors; German Version DIN EN ISO 22477-5:2018*. ISO, (2019).

[5] European Committee for Standardization. *EN 1537:2013: Execution of special geotechnical works - Ground anchors; German version EN 1537:2013*. Berlin. (Juli 2014).

[6] DIN Deutsches Institut fuer Normung. *Supplementary provisions to DIN EN 1537:2014-07, Execution of special geotechnical works - Ground anchors*. Berlin.(November 2017).

[7] European Committee for Standardization. *EN 1997-1 Eurocode 7: Geotechnical design - Part 1: General rules; German version EN 1997-1:2014*. Berlin. (2014).

[8] DIN Deutsches Institut fuer Normung. *Subsoil - Verification of the safety of earthworks and foundations - Supplementary rules to DIN EN 1997-1*. Berlin. (April 2021).

[9] Ang, A.H.S. and Tang, W.H., *Probability Concepts in Engineering: Emphasis on Applications to Civil and Environmental Engineering*. 2nd Edition, Wiley, New York. (2007).

[10] Baecher, G.B., Christian J.T. *Reliability and Statistics in Geotechnical Engineering*. John Wiley & Sons Ltd, Chichester (2003).

[11] Beer, M., Zhang, Y., Quek, S.T., Phoon, K.-K. Reliability analysis with scarce information: Comparing alternative approaches in a geotechnical engineering context. *Structural Safety*. (2013) **41**:1–10.

[12] Phoon, K.-K., Kulhawy, F.H. Characterization of geotechnical variability. *Can. Geotech. J.*. (1999) **36**:612–624.

[13] Jiang, S.-H., Papaioannou, I., Straub, D. Optimization of Site-Exploration Programs for Slope-Reliability Assessment. *ASCE-ASME Journal of Risk and Uncertainty in Engineering Systems, Part A: Civil Engineering*. (2020) **6**(1).

[14] Cao, Z.-J., Wang, Y., Li, D.-Q. Site-specific characterization of soil properties using multiple measurements from different test procedures at different locations - A Bayesian sequential updating approach. *Engineering Geology*. (2016) **211**:150–161.

[15] Papaioannou, I., Straub, D. *Learning soil parameters and updating geotechnical reliability estimates under spatial variability - theory and application to shallow foundations*. Georisk: Assessment and Management of Risk for Engineered Systems and Geohazards. (2017) **11**(1):116–128.

[16] Jiang, S.-H., Papaioannou, I., Straub, D. Bayesian updating of slope reliability in spatially cariable soils with in-situ measurements. *Engineering Geology*. (2018) **239**:310–320.

[17] Cheung, S.H., Oliver, T.A., Prudencio, E.E., Prudhomme, S., Moser, R.D. Bayesian uncertainty analysis with applications to turbulence modeling. *Reliability Engineering and System Safety*. (2011) **96**:1137–1149.

[18] Zhang, J., Zhang, L.M., Tang, W.H. Bayesian Framework for Characterizing Geotechnical Model Uncertainty. *Journal of Geotechnical and Geoenvironmental Engineering*. (2009) **135**(7):932–940.

[19] Shi, Y., Xu, P., Peng, J., *An Overview of Adjustment Methods for Mixed Additive and Multiplicative Random Error Models*. In: International Association of Geodesy Symposia, Rome, 2013, pp. 283–290.

[20] Hoff, P.D. and Niu, X. A Covariance Regression Model. *Statistica Sinica*. (2012) **22**:729–753.

[21] Gelman, A., Carlin, J.B., Stern, H.S., Dunson, D.B., Vehtari, A., Rubin, D.B. *Bayesian Data Analysis*. 3rd Edition, Chapman and Hall/CRC. . (2013).

[22] Montero-Cubillo, N.S., Galindo-Aires, R.A., Serrano-González, A., Olalla-Marañón, C., and Simic-Sureda, F.D. Analytical Model of an Anchored Wall in Creep Soils. *International Journal of Geomechanics*. (2020) **20**(4).

[23] Hoffman, M.D., Gelman, A. *The No-U-Turn Sampler: Adaptively Setting Path Lengths in Hamiltonian Monte Carlo*. arXiv:1111.4246. (2011).

[24] Betz, W., Papaioannou, I., Straub, D. Bayesian post-processing of Monte Carlo simulation in reliability analysis. *Reliability Engineering and System Safety*. (2022) **227**.